Available online at www.sciencedirect.com
SCIENCE DIRECT
Engineering Failure Analysis 11 (2004) 561–573
ENGINEERING FAILURE ANALYSIS
www.elsevier.com/locate/engfailanal

Impact failure analysis of re-circulating mechanism in ball screw

Jui-Pin Hung[a], James Shih-Shyn Wu[b,*], Jerry Y. Chiu[c]

[a]*Department of Mechanical Engineering, Nanya Institute of Technology, 414, Sec. 3, Jung-Shan E. Road, Chungli, Taiwan 320, Taiwan, ROC*
[b]*Institute of Mechanical Engineering, National Chung-Hsing University, 250, Kuo-Kuang Road, Taichung, Taiwan 402, Taiwan, ROC*
[c]*Department of Product R&D, Hiwin Technologies Corporation, 46, 37th Road, Taichung Industrial Park, Taichung, Taiwan 407, Taiwan, ROC*

Received 23 August 2003; accepted 27 September 2003

Abstract

A ball screw driven mechanism is a major component in high-speed/high-precision transmitting systems. In such a mechanism, the return tube has been designed to provide the path for a steel ball rolling in screw grooves. As the driven shaft in the mechanism operates at high rotating speed, forces caused by the impact activity between the steel ball and return tube may generate high stresses and cause damage to the return tube after some significant service times. In order to understand the fracture conditions in the return tube, an impact-contact formula is developed and the transient behavior is investigated based on the finite element method in this paper. From results obtained here, it is shown that the rotational speed of the ball screw may affect the service life of the return tube significantly. Factors that affect the service life of the re-circulating mechanism are then described in detail. Further suggestions for the improvement of the return tube in the design/fabrication processes are also proposed in the final part of this paper.

Keywords: Contact forces; Fatigue failure; Impact; Mechanical components; Transmission systems

1. Introduction

A ball screw driven mechanism is a major component in the development of high-speed/high-precision transmitting systems. Under the requirement for high-speed transmitting systems such as the recent applications in semiconductor fields, the feed rate of the ball screw is faster than 80 $\mathrm{m\,min^{-1}}$, which is much higher than the conventional rate, 30 $\mathrm{m\,min^{-1}}$ or lower. Generally speaking, the requirement of high feed rate can be reached by increasing the rotational speed of the ball screw. However, the maximum rotational speed is restricted by the allowable $d_m N$ value (product of ball pitch circle diameter d_m in mm and

* Corresponding author. Tel.: +886-4-22840433; fax: +886-4-22877170.
E-mail address: sswu@dragon.nchu.edu.tw (J. Shih-Shyn Wu).

1350-6307/$ - see front matter
doi:10.1016/j.engfailanal.2004.01.002

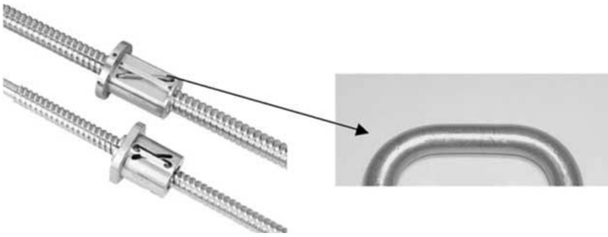

Fig. 1. Ball screw with outer re-circulating mechanism, and appearance of return tube.

rotational speed N in rpm) of the ball screw in the design process. Current standard d_mN values for ball screws designed under certain specifications are defined within the range from 70,000 to 80,000 [1]. For a ball screw with diameter 50 mm and leading pitch 20–30 mm operating at rotational speeds of 2000–3000 rpm, a higher feed rate is reached but with a d_mN value of 100,000–150,000 exceeds the standard rated values. The high rotational speed of the ball screw also bring some annoying problems such as the failure of the re-circulating mechanism, thermal deformation due to high operating temperature and higher levels of vibration and noise, which are not seen under conventional operating conditions. Among these problems, failures of re-circulating mechanisms are observed to occur by structural fracture of components. Especially the return tube, which is designed to provide the path for steel balls rolling in screw grooves, usually endures the repeated impact loadings generated by steel balls. Consequently, fracture of the return tube is considered in the design of ball screws withstanding high d_mN values.

In engineering applications, the occurrence of fatigue failure is related to material flaws and manufacturing defects, but it is often initiated for mechanical reasons; in particular, the cyclic stress induced in structural members is well recognized as the main cause for fatigue failures. Generally the fatigue process consists of two stages, crack initiation and crack growth [2]. Stress concentrations often cause plastic strains to accumulate in a local area and lead to crack initiation after long-term repeated loadings. Once the microcracks are initiated, they will propagate within the component when the cyclic stresses are raised to sufficient levels. For the mechanical component studied in this paper, the inlet of the return tube is machined into a shape like a tongue (Fig. 1) so that it can guide the balls flowing into the return tube more easily. Owing to the discontinuity in geometric features, microcracks are expected to originate from the root notch of the tongue under cyclic loading and fatigue fracture is prone to occur in subsequent service. This will finally result in the malfunction of the ball screws.

The goal of this paper is aimed at investigating the impact induced failure of the return tube by means of mechanical analysis. For this purpose, the impact-contact formula is first employed to calculate the impact force generated by the interaction between the return tube and the steel ball. Next, transient stress analysis based on the finite element method is performed to investigate the dynamic responses of the return tube under impact excitations. Finally, the fatigue lifetimes under various service conditions are estimated using appropriate failure criteria. Through the proposed model, the operating conditions leading to the damage of the return tube are discussed. This might contribute to improvements for future design of the re-circulating mechanism of ball screw systems.

2. Basic theory

2.1. Impact contact formula

Fig. 2 is a schematic illustrating a steel ball flowing into the return tube. The contact between the inlet of the return tube (or the tongue) and the ball is modeled as an equivalent model of a sphere contacting a

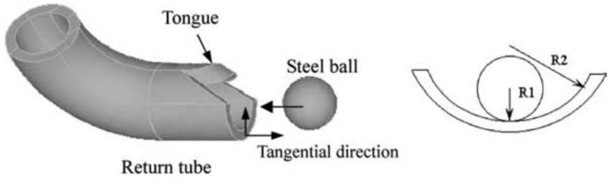

Fig. 2. Schematic for steel ball flowing into the return tube. The contact status between ball and tongue is modeled as a sphere contacting with cylindrical concave surface.

cylindrical concave surface (Fig. 2). At any instant the contact force can therefore be determined by utilizing the Hertzian contact law of the form [3].

$$F = k_{\mathrm{h}}\alpha^{3/2}, \tag{1}$$

where α is the normal deformation, and k_{h} is the Hertzian stiffness which depends on the material properties and contact geometry. The Hertzian stiffness can be determined from

$$\begin{aligned} k_{\mathrm{h}} &= \frac{4}{3}\frac{q_k^{3/2}}{(\delta_1+\delta_2)\sqrt{(A+B)}}, \\ \delta_i &= \frac{1-\mu_i^2}{\pi E_i} \quad i = 1, 2, \end{aligned} \tag{2}$$

where μ and E are the Poison's ratio and Young's modulus of the contact bodies respectively. A, B and q_k are geometrical constants defined by the curvature radii R_1 and R_2 of spherical and concave cylindrical surfaces, as given below.

$$A = \frac{1}{2}\left(\frac{1}{R_1} - \frac{1}{R_2}\right), \quad B = \frac{1}{2R_1}, \tag{3}$$

and q_k is expressed as a function of A/B. More details are given in [3].

Since the ball collides with the return tube instantaneously at high velocity, the impact force acting on contacting bodies will vary with time during contact duration. At this moment, the impact force acting on each body can further be derived according to Newton's second law and given by following equation [4],

$$F = -m_1\ddot{w}_1 = -m_2\ddot{w}_2 = -\frac{m_1 m_2}{m_1+m_2}\ddot{\alpha}, \tag{4}$$

where $\ddot{\alpha} = \ddot{w}_1 + \ddot{w}_2$ represents the acceleration of the center of the two impact bodies with mass m_1 and m_2, respectively. $\ddot{w}_1$ and $\ddot{w}_2$ are the accelerations of the two bodies and F is the contact force given in Eq. (1).

Substituting Eq. (1) into Eq. (4), yields

$$\begin{aligned} \ddot{\alpha} &= -k_1 k_{\mathrm{h}}\alpha^{3/2}, \\ k_1 &= (m_1+m_2)/m_1 m_2. \end{aligned} \tag{5}$$

Taking the integration of Eq. (5) with the initial conditions $\alpha(0) = 0$, $\dot{\alpha}(0) = V_0$, the relative velocity at instant of collision, we have

$$\frac{1}{2}(\dot{\alpha}^2 - V_0^2) = -\frac{2}{5}k_1 k_\mathrm{h}\alpha^{5/2}. \tag{6}$$

Since the maximum deformation α_m at the contact point occurs at the instant of zero relative velocity, hence

$$\alpha_\mathrm{m} = \left[\frac{5V_0^2}{4k_1 k_\mathrm{h}}\right]^{2/5}. \tag{7}$$

Integrating the term $\dot{\alpha}$ in Eq. (6), and rearranging, we have the following formula for impact force as a function of time.

$$F = \frac{1.140V_0^2}{k_1\alpha_\mathrm{m}}\sin\left(\frac{1.068V_0}{\alpha_\mathrm{m}}\right)t \quad \text{for } 0 \leqslant t \leqslant \frac{\pi\alpha_\mathrm{m}}{1.068V_0}. \tag{8}$$

2.2. Governing equation for dynamic response

Equations that govern the dynamic response of the return tube subjected to dynamic forces can be derived from D'Alembert's principle and written into the finite element formulation.

$$[M]\{\ddot{d}\} + [C]\{(\dot{d}\} + [K]\{d\} = \{F^\mathrm{ext}\}, \tag{9}$$

where $[M]$, $[C]$ and $[K]$ are the mass matrix, damping matrix and stiffness matrix of the whole structure, respectively. $\{d\}$, $\{\dot{d}\}$ and $\{\ddot{d}\}$ are the system nodal displacement, velocity and acceleration, respectively. $\{F^\mathrm{ext}\}$ is the force vector including the impact force between the return tube and the steel ball.

Since the contact duration is very short, the impact force acting on the tongue can be referred to as an impulse of the form $F = \lim_{\Delta t \to 0}(m\Delta v/\Delta t) \approx \infty$. For mechanical components subject to the impact excitation, the effect of the stress wave propagating within the material is of great importance in the analysis, in particular for structural members with higher natural frequency. The stress wave will cause the stress distribution in mechanical components to vary with time and bring the stress to higher levels than that induced under static contact loading. For the solution of Eq. (9), the direct integration by the trapezoidal rule method [5] is implemented in the finite element algorithm and hence the time-history of the impact stress can be obtained.

2.3. Finite element modeling

According to the specification of a ball screw with nominal diameter of 55 mm, the diameter of steel ball is 6.350 mm, and the return tube has an outer diameter of 9.2 mm and an inner diameter of 6.85 mm. Referring to the assembly of the return tube mounted in the nuts of the ball screw, two three-dimensional finite element models were created, as shown in Fig. 3. These models were fine meshed with hexahedron brick elements to consider the geometric attributes around the root of the tongue. Model I is the main segment of the return tube including the tube inlet for the steel ball and is used for the evaluation of impact force and overall stress state within the return tube during impact. Considering the efficiency of transient stress analysis, model I was simplified into model II with appropriate constraints. Both the ball and return tube are fabricated from SUS304 stainless steels with material properties [6]: Young's modulus $E = 190$ GPa, Poisson's ratio $\nu = 0.305$, density $\rho = 760$ kg/m^3, yield strength $\sigma_\mathrm{y} = 271$ MPa and ultimate tensile strength $\sigma_\mathrm{ut} = 627$ MPa.

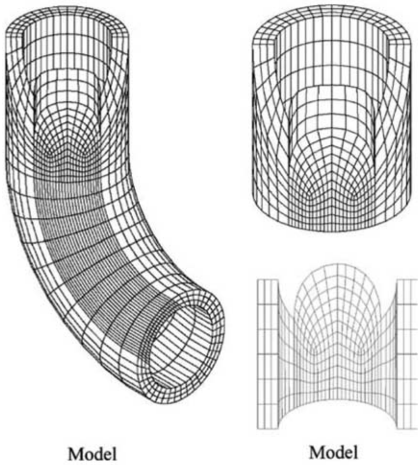

Fig. 3. Finite element model of return tube with inner view of tongue. Model I: main segment of tube with 4072 nodes and 2904 elements. Model II: inlet of tube with 1832 nodes and 1224 elements.

3. Results and discussion

3.1. Solution for impact force

To reduce the complexity encountered in real contact between the return tube and the steel ball, two assumptions were made before the calculation of impact force. First, the effect of sliding friction on contact force was ignored. Second, for each ball colliding the return tube, the tangential deformation at the contact zone was smaller than the deformation in the normal direction, and hence the impact effect in tangential direction was neglected. Under these assumptions, only the normal contact force was considered and thereby the maximum impact force induced at each collision could be calculated from Eqs. (7) and (8) by replacing V_0 with V_n, the normal component of the impact velocity of the steel ball. That is,

$$F = \frac{1.140 V_{\mathrm{n}}^2}{k_1 \alpha_{\mathrm{m}}}, \qquad \text{where } \alpha_{\mathrm{m}} = \left[\frac{5 V_{\mathrm{n}}^2}{4 k_1 k_{\mathrm{h}}}\right]^{2/5}, \quad V_{\mathrm{n}} = \frac{\pi D N}{60} \sin\theta. \tag{10}$$

In the above equation, D and N are the nominal diameter and rotational speed of the ball screw respectively. θ is the impact angle of the steel ball flowing into the return tube, which is measured from the tangential direction. Actually, the steel balls flow into the return tube nearly along the tangential direction at tube inlet when escaping from the screw shaft, and hence the impact angle may vary randomly in a narrow range. By substituting all relating data into Eq. (10), the impact forces were then determined.

For ball screws with basic specifications: nominal diameter $D = 55$ mm, ball diameter $d = 6.35$ mm, variations of the impact forces with the rotational speeds of the screw shaft are shown in Fig. 4, and were assessed under different impact angles respectively. Current results are fully consistent with the measured data (Fig. 5) available in NSK technique report [1]. Comparison of these results leads to the conclusion that the equivalent contact model proposed here is an adequate representation of the contact between return tube and steel balls in the re-circulating mechanism. From Fig. 4, it is known that the impact forces generated at a rotational speed of 2000 rpm vary from 51 to 67 N, depending on the impact angle that is

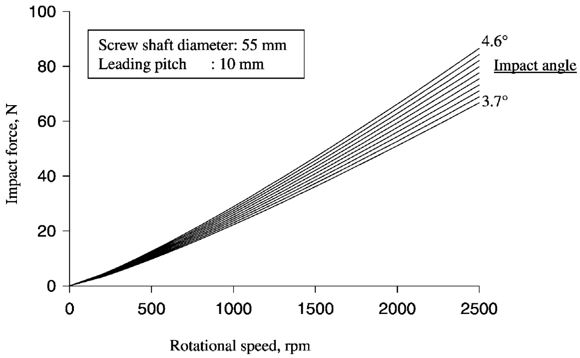

Fig. 4. Predicted impact forces at various rotational speeds. The impact angles range from 3.7° to 4.6°.

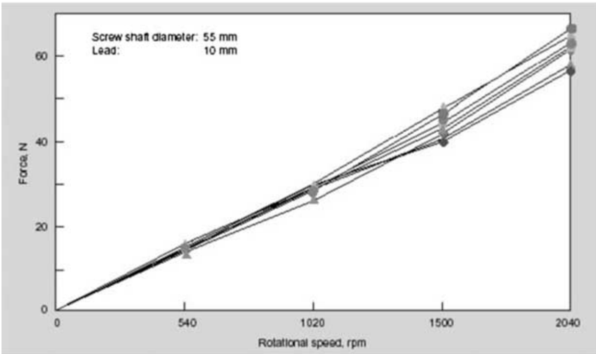

Fig. 5. Measured impact forces at various rotational speeds, extracted from NSK technology report [1].

expected to vary within the range of 3.7–4.6° for each steel ball hitting the return tube. For a ball screw with the other specification ($D = 41.5$ mm, $d = 6.35$ mm), the impact force corresponding to different rotational speeds is shown in Fig. 6. It indicates that the impact forces fall within in the range of 36–47 N when the screw shaft rotates at 2000 rpm. These impact forces were then applied in the FE model for subsequent stress analysis by using the finite element program FEAST[1].

3.2. Transient stress analysis

In order to get insight into the stress distributions around the tongue of the return tube, static stress analyses were first performed, in which the maximum force of 47 N generated at a speed of 2000 rpm was applied to the local area at the tip of the tongue, instead of a point load. The loading area can be estimated from Hertzian contact law [3]. Fig. 7 shows the pattern of stress distribution induced in the tongue. As seen in Fig. 7, the root notches of the tongue are the critical regions with a remarkable stress concentration. The geometrical effect of the tongue is significant. The maximum principal stress at a rotational speed of 2000 rpm is 277 MPa, which is slightly greater then the yield strength, but well below the ultimate tensile strength of the material. Next, further investigation of the impact effect on stress level was made through

[1] FEAST-Finite Element Analysis of Structures. 1993, a software package enters the information storage and retrieval of literature reference of the database of the system MAKEBASE developed by J.S.S. Wu. and distributed by Department of Mechanical Engineering, Linkoping Institute, Sweden.

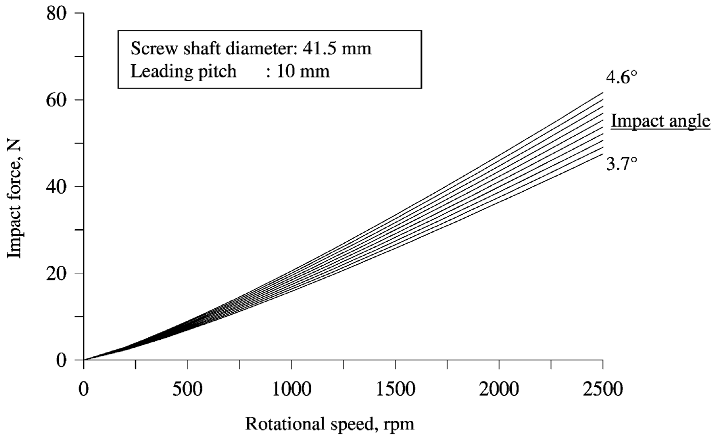

Fig. 6. Predicted impact forces at various rotational speeds. The impact angles range from 3.7° to 4.6°.

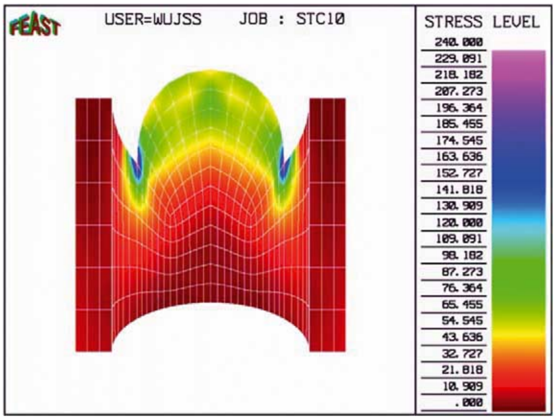

Fig. 7. Stress distribution within tongue of return tube (von-Mises stress unit: MPa, which was derived under static loading mode for ball screw speed 2000 rpm, impact angle = 4.6°).

the transient analysis. Before this, the modal analysis was performed to examine the possible dynamic behavior of the return tube under impact excitations. The results of modal analysis reveal that this component has the first bending vibration mode with the fundamental frequency of 9620 Hz (Fig. 8). It is worth noting that the first modal shape appears like the impact excitation in bending induced by the collision of steel balls, which is believed to be a substantial contributor to the occurrence of fatigue failure of the return tube. This phenomenon was verified from the results of transient analysis and subsequent failure analysis. In transient analysis, the maximum impact forces generated under various operating conditions were applied to the tongue model to yield the expected highest stress levels. The time history of the impact stress induced at the root notch of the tongue is shown in Fig. 9. In the figure, it can be seen that the impact stresses reached peak values almost at the same time for various rotational speeds. Fig. 10 further demonstrates the stress wave propagation within the tongue of the return tube. Comparison of the stresses predicted under impact and static modes is shown in Fig. 11. At a certain screw speed, the predicted maximum impact stresses at the root notch are higher than those generated under the static mode, by approximately 1.58 times. Current results show that the rotational speed of the ball screw has a prominent

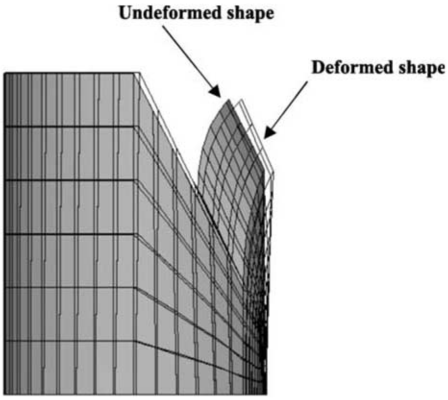

Fig. 8. Fundamental mode shape in bending (gray shaded image: undeformed shape, wire frame: deformed shape).

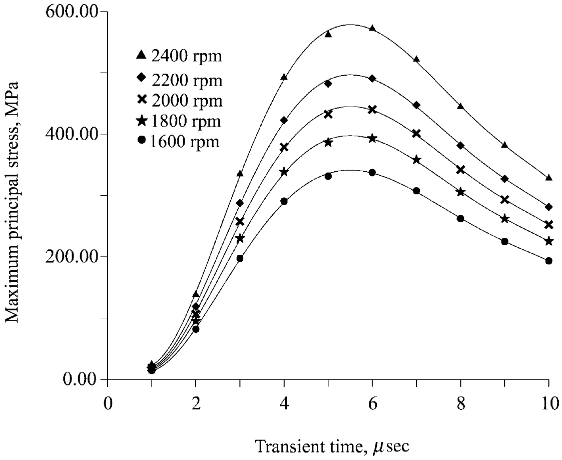

Fig. 9. Time history of maximum principal stress for various operating speeds (derived under impact contact mode, impact angle = 4.6°).

influence on the stress levels in the tongue. In addition, owing to the inertial effect from impact contact, the stress wave propagating in the tongue has resulted in higher stress.

3.3. Failure analysis

As revealed in the stress analysis, when the ball screw operates at a speed over 1600 rpm, the maximum tensile stresses induced in the tongue are higher than the yield strength (271 MPa) of the material, but still lower than the ultimate tensile strength (627 MPa). Such an impact effect is apparently enhanced with the increase of operating speed of the ball screw. Besides, the impact stress is generated repetitively since the steel balls are driven to collide with the return tube in succession by the screw shaft. Furthermore, it also has non-reversed cyclic characteristics due to the propagation of the stress wave in the structure.

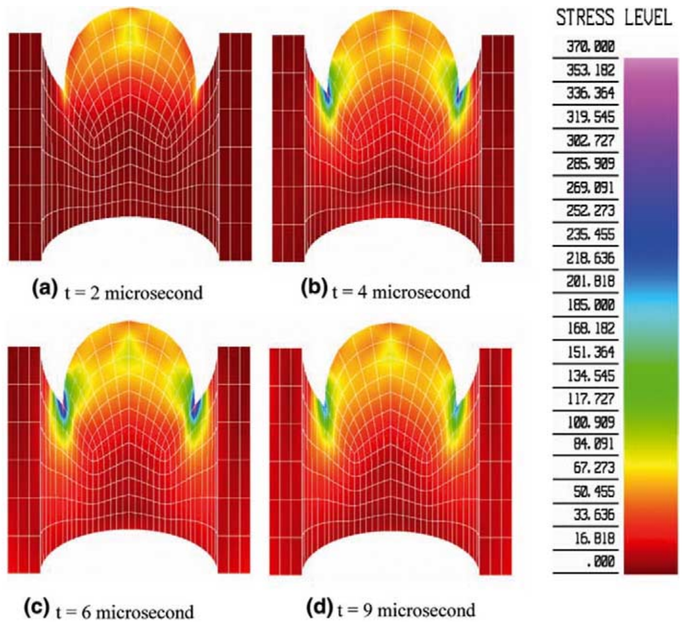

Fig. 10. Shaded image illustrating stress propagation within tongue of return tube (von-Mises stress unit: MPa, predicted under impact loading induced at screw speed of 2000 rpm, impact angle = 4.6°).

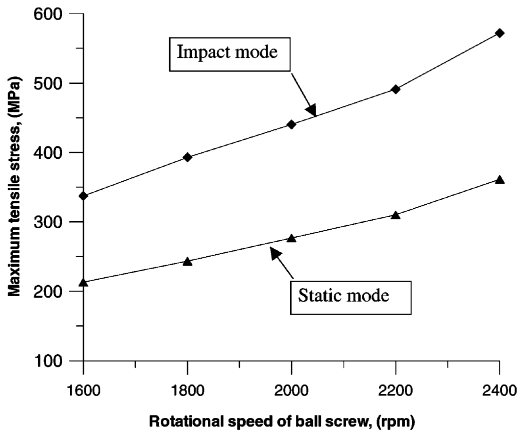

Fig. 11. Predicted maximum tensile stresses within tongue for various rotational speeds of ball screw. These stresses are assessed under static and impact modes respectively, showing the impact effect on stress.

For components subjected to fully reversed cyclic stress, Basquin's power law [7] based on the stress-life method was commonly adopted to assess the fatigue lifetime, that is

$$A = \sigma_R N_R^B, \tag{11}$$

where σ_R is the cyclic stress, N_R is the fatigue lifetime, and the constants A and B are related to the material strengths. A and B can be determined from

$$A = \frac{(0.9\sigma_{ut})^2}{\sigma_e}, \quad B = \frac{1}{3}\log\left(\frac{0.9\sigma_{ut}}{\sigma_e}\right) \tag{12}$$

in which σ_e and σ_{ut} are endurance limit and ultimate strength of material respectively. Usually the endurance limit σ_e can be derived from the S–N curve (Fig. 12). In this paper, this value is 284 MPa for the SUS304 stainless steel used for the return tube [6].

However, in the case of non-reversed cyclic stresses, in order to consider the mean stress effect on fatigue lifetime, the stress state with stress amplitude σ_r and mean stress σ_m should be converted into equivalent fully reversed stresses by using the Goodman failure criterion [8],

$$\sigma_R = \frac{\sigma_r \sigma_{ut}}{\sigma_{ut} - \sigma_m}. \tag{13}$$

When the screw shaft rotated at 2000 rpm, the principal stresses induced at the root notch of the tongue increased from a minimum value σ_{min} of 0 MPa to a maximum value σ_{max} of 440 MPa at each impact cycle. The equivalent fully reversed stress was estimated to be 359 MPa from Eq. (13), which obviously exceeds the endurance limit, and hence fatigue failure occurred after certain number of impact cycles. This finite lifetime N_R was estimated to be 6.36×10^4 cycles using Basquin's power law. It was worth noting that such a lifetime was predicted under the critical stress status where the maximum impact force was applied in the FE model. However, as stated in the previous paragraphs, the impact angle of steel balls might vary within the range 3.7–4.6°, which would bring the impact forces and stresses to different values. Realistically, it is uncertain that the impact stress induced at each collision is sufficiently higher to initiate such a failure. As a consequence, the estimated lifetimes are regarded as conservative values, representing the effective impact cycles that can substantially contribute to the initiation of fracture at the notch of the tongue.

Table 1 summarizes the maximum tensile stress, equivalent fully reversed stress and impact cycles to failure of the return tube under various rotational speeds of the ball screw. As expected, the rotational speed of the screw shaft has profound effect on the fatigue lifetime of the return tube. In addition, it can be seen from Table 1 that the critical speed for safe running in service is 1800 rpm, which yields approximately one million impact cycles for the failure to initiate. It is noted that the equivalent $d_m N$ value is approximately

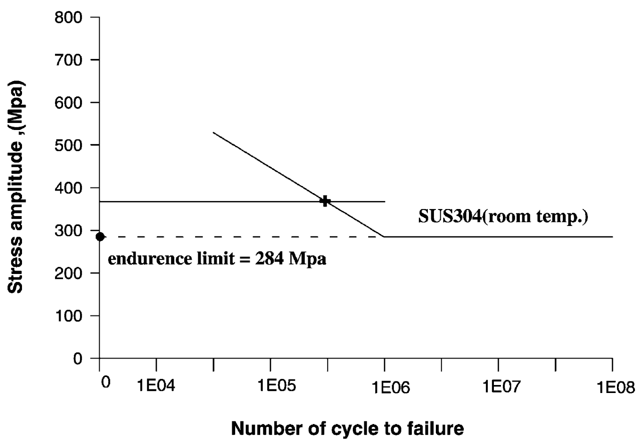

Fig. 12. S–N curve for SUS304 stainless steel [6].

Table 1
Comparison of the maximum tensile stress and fatigue lifetime predicted under various operating speeds of ball screw

Operating speed (rpm)	σ_{max} (MPa)	σ_R (MPa)	N_R(cycle)
1000	192.7	114	9.37×10^9
1200	239.2	147	7.53×10^8
1400	288.3	189	6.00×10^7
1600	337.3	230	8.34×10^6
1800	392.9	285	0.96×10^6
2000	440.0	339	1.68×10^5
2200	490.3	402	3.00×10^4
2400	571.9	526	2.00×10^3

72,000. This is consistent with the currently guaranteed d_mN values. As revealed in the current results, the d_mN value obviously limits the safe operating speed of the ball screw.

3.4. Design implications

In the failure analysis, the fatigue lifetime was estimated based on the stress-life method. This method was developed according to the empirical relationships obtained from the standard fatigue tests. The true stress–strain behavior was ignored under the assumption of fully elastic strains in material. However, current results show that the impact stresses induced at the root notch may exceed the yield strength when the ball screw rotates at higher speed. It is shown that microcracks will be initiated owing to the accumulation of local plastic strains and propagate to final fracture under repetitive impact loadings. Under such situations, the strain-life approach coupled with fracture mechanics seems to be more adequate for further investigation of the fracture behavior of return tubes in more realistic ways. Even then, the current results elucidate the failure causes of the re-circulating mechanism and suggest constraints on the development of

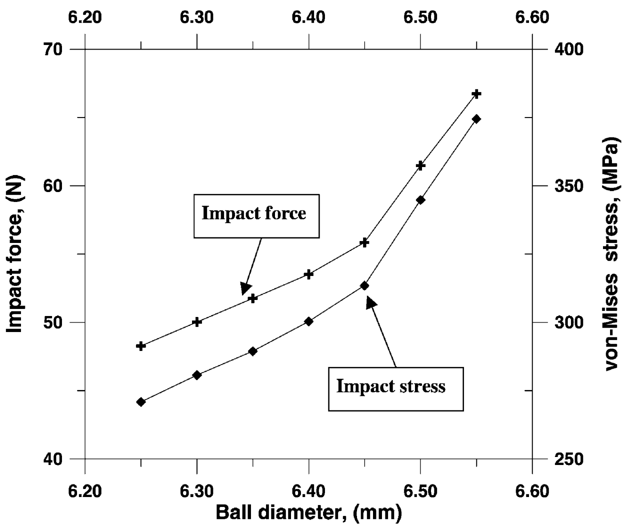

Fig. 13. Impact forces and impact stresses induced within return tube as a function of ball diameter (screw shaft diameter = 41.5 mm, standard ball diameter = 6.35 mm).

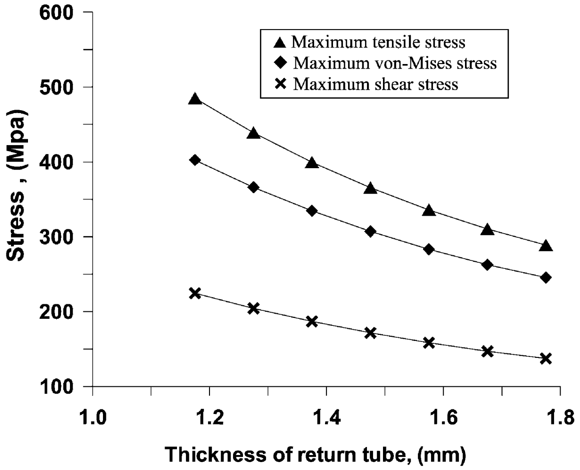

Fig. 14. Impact stresses induced within return tube as a function of wall thickness of return tube (screw shaft diameter = 41.5 mm, standard ball diameter = 6.35 mm, inner diameter of return tube = 6.85 mm, keep unchanged).

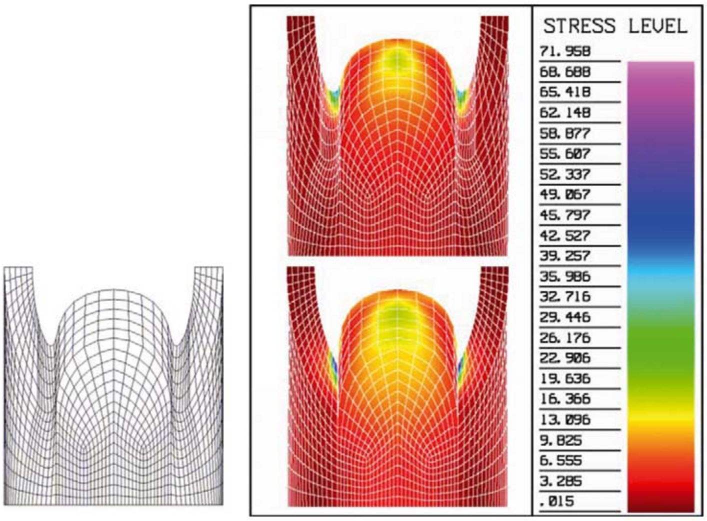

Fig. 15. (a) New tongue model with blunt notches at root, fillet radius = 1.0 mm. (b) Comparison of von-Mises stress distributions for tongues with sharp notch and blunt notch. The stresses were predicted under unit impact force.

high $d_m N$ values for ball screw systems. This essentially can be ascribed to poor design in the entry of the return tube.

The impact force generated by the steel ball also plays an important role in fatigue lifetime of the return tube. As revealed in the impact-contact formula, the impact force is governed by the Hertzian contact stiffness k_h, mass constant k_1 and impact velocity V. These factors are related to the design parameters in component dimensions such as diameter of screw shaft, steel ball or return tube. By further comparison of the results in Fig. 4 and 6, it is found that under the same operating condition a thicker screw shaft will drive the ball to higher revolving speed and generates larger impact forces and high stress levels on the return tube. This shows that the $d_m N$ value, representing the revolving speed of the ball, dominants the fatigue lifetime of ball re-circulating mechanisms. Fig. 13 demonstrates how the impact force and stress are influenced by the diameter of the steel ball, in which the ball diameter is changed within the constraint of the inner diameter of return tube. Apparently, a steel ball with a smaller diameter reduces the impact effect on the return tube and hence the risk of failure, however this may lower the load-carrying capacity of the ball screw. On the other hand, an increase in the wall thickness of the return tube slightly affects the impact force (less than 3% approximately), but significantly reduces the impact stresses (Fig. 14). An increase in fatigue lifetime also can be expected by improving the geometry features at the root notch with adequate fillet radius to lessen the stress concentration. As shown in Fig. 15, a new tongue model with blunt notches (fillet radius = 1.0 mm) was constructed and the maximum stress at notches was greatly reduced, approximately 30% less than that generated in the original model with sharp notches.

The other factors affecting the failure behavior of return tubes can further be clarified from the proposed model. It is believed that this work has provided directions for the improvement in the design or fabrication of re-circulating mechanisms to satisfy the demand for high $d_m N$ ball screw systems.

4. Conclusions

In this paper, an equivalent contact model associated with the impact contact theory was employed to determine the impact forces exerted on return tubes by the hitting of steel balls. The proposed model was proved to be successful in simulating such an impact contact behavior when compared with the measured data available in the literature. Further analyses of impact response indicated that higher stresses were induced at the root notch of the tongue. This was considered as the initiation of fatigue failure owing to the impact bending excitation with cyclic characteristics. Results of failure analysis also showed that the rotational speed of the screw shaft affected the lifetime of return tubes in service, which eventually illustrates the limit of the rated $d_m N$ value on the operating conditions of ball screws. The prevention of failure and the goal of increasing $d_m N$ values of ball screws can be also achieved through ways such as increasing the wall thickness of the return tube to reduce stress level, redesigning the tongue geometry of the return tube to avoid stress concentrations, or using higher grades of materials in fabrication.

Acknowledgements

The authors acknowledge the financial support of the Hiwin Technologies Corp.

References

[1] Ninomiya M, Miyaguchi K. Recent technical trends in ball screws. NSK Tech J: Motion Control 1998;664:1–3.
[2] Dowling NE. Fatigue at notches and the local strain and fracture mechanics approaches. In: Fracture Mechanics, ASTM STP 677, American Society for Testing and Materials, Philadelphia, 1979. p. 247–73.
[3] Goldsmith W. Impact: the theory and physical behavior of colliding solids. London: Edward Arnold Ltd; 1960 p. 82–90.
[4] Johnson KL. Contact mechanics. Cambridge: University of Cambridge; 1985 p. 351–5.
[5] Cook RD, Malkus DS, Plesha ME. Concepts and application of finite element analysis. New York: John Wiley and Sons; 1988 p. 405–7.
[6] Nishida SI. Failure analysis in engineering application. London: Buttterworth-Heinemann Ltd; 1992 p. 61–5.
[7] Basquin OH. The exponential law of endurance tests. Am Soc Test Mater Proc 1910;10:625–30.
[8] Hertzberg RW. Deformation and fracture mechanics of engineering materials. New York: John Wiley and Sons; 1996 p. 530–2.